Transportation Geotechnics 37 (2022) 100845

Contents lists available at ScienceDirect

Transportation Geotechnics

journal homepage: www.elsevier.com/locate/trgeo

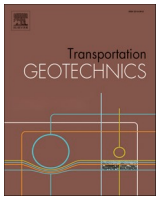

The effect of rolling stock characteristics on differential railway track settlement: An engineering-economic model

C. Charoenwong [a], D.P. Connolly [a], K. Odolinski [b,f], P. Alves Costa [c], P. Galvín [d,e], A. Smith [b]

[a] Institute for High Speed Rail and Systems Integration, School of Civil Engineering, University of Leeds, UK
[b] Institute for Transport Studies, University of Leeds, UK
[c] Faculty of Engineering, University of Porto, Portugal
[d] Escuela Técnica Superior de Ingeniería, Universidad de Sevilla, Camino de los Descubrimientos s/n, 41092 Sevilla, Spain
[e] Laboratory of Engineering for Energy and Environmental Sustainability, Universidad de Sevilla, Camino de los Descubrimientos s/n, 41092 Sevilla, Spain
[f] The Swedish National Road and Transport Research Institute (VTI), Malvinas väg 6, Box 55685, SE-102 15, Stockholm, Sweden

ARTICLE INFO

Keywords:
Railway track geometry
Railroad track tamping
Marginal railway cost
Freight heavy haul
Rolling stock linespeed
Railway operation economics

ABSTRACT

Railway track geometry deteriorates under repeated train loading. When linespeed is increased or new rolling-stock is introduced this can alter the future rate of change of differential settlement and track geometry. Therefore this paper presents a novel combined engineering-economic approach to investigate the effect of increasing train speeds, adding additional passenger movements, and adding additional freight movements to an existing line. Firstly a numerical algorithm is presented to compute differential track settlement. An important novelty of the model is its use of the wavenumber finite element method coupled with settlement relationships in a manner that allows for track irregularities to evolve after every load passage (i.e. taking into account the evolution of the track unevenness profile before applying each subsequent train passage). Unlike traditional approaches this allows the model to faithfully simulate mixed traffic conditions, including the coupled interactions between different rolling stock types and track geometry. The engineering model is used to predict tamping intervals, and then coupled with an economic model capable of calculating deterioration elasticities and marginal costs. It is shown that higher speeds result in higher dynamic forces and cause a faster rate of deterioration of track geometry, thus increasing marginal cost. The model is then used to investigate the effect of adding additional train movements to a passenger line. It is shown that additional movements increase the rate of track degradation and marginal costs, particularly if the additional traffic is freight. This is because freight vehicles typically have one only layer of (stiff) suspension, thus generating elevated dynamic forces compared to passenger vehicles.

Introduction

Under repeated train passages, railway tracks settle differentially along the line due to dynamic train-track interaction and changing track support conditions [1]. Deterioration in vertical track geometry results in a cycle of increased train-track dynamic interaction forces and further track deterioration. These track irregularities evolve with each load passage, meaning the characteristics of the train-track dynamic interaction forces, track stress distributions and the settlements also evolve over time. If each track section is subject to relatively constant operational conditions (i.e. no significant changes to rolling stock types, speeds and timetables), and no heavy maintenance/renewal is performed, then future track geometry changes can be approximated by extrapolating from historical data, with minimal regard for the underlying physics of track degradation [2–7]. This means variables such as changes in train-track interaction and track stress distributions can be ignored.

Although useful for routine cases, if a railway operator wishes to increase linespeed, or increase the annual number of rolling stock movements (either freight or passenger), maintenance frequency prediction using statistical extrapolation of historical records becomes more difficult because experimental data to perform forecasting analysis is not available. This then introduces uncertainties into marginal cost calculations, and thus the operator's economic appraisal. An important driver behind operational cost is track maintenance frequency. To predict future maintenance intervals requires modelling of operational conditions that are different than the past.

Rather than a statistical approach, this task is well suited to numerical modelling from first principles, where arbitrary future operational conditions can be simulated without relying on past track geometry records. This approach has been studied by [8–11], where an iterative train-passage simulation approach combined with settlement models is used to compute differential settlement, considering changes

https://doi.org/10.1016/j.trgeo.2022.100845
Received 23 May 2022; Received in revised form 16 August 2022; Accepted 18 August 2022
Available online 24 August 2022

in track geometry. However, modelling cyclic loading in the time domain demands significant computational effort, and is thus challenging when calculating the 3D dynamic stress fields in the track and ground over a large number of loading cycles [12–16]. It is also important that the distribution of track-ground stresses is modelled explicitly because the deviatoric stress is one of the most influential parameters when computing settlement [17].

Two fundamental parts of a settlement prediction model are first calculating the stress/strain response of the structure, and secondly calculating the corresponding settlement. Regarding settlement calculation, two common modelling approaches for calculation are constitutive [18–23] and empirical [17,24–32]. The constitutive approach often requires higher computational effort and a non-trivial number of material input properties that are difficult to quantify, thus making real-life application challenging [33,34]. An alternative modelling approach is to use empirical equations which have fewer input parameters and require minimal computation, yet if used with care, can provide similar accuracy to constitutive models [35].

Most railway administrations use a track quality index (TQI) to measure track quality. Although many TQI variants exist [36], the standard deviation (SD) of vertical track geometry over a given track length is the most commonly used [37]. When the SD value, for wavelengths within a given range, exceeds a threshold limit (which is linked to linespeed), maintenance action is required. Tamping is then the most common corrective maintenance technique to restore the track geometry to an acceptable level of quality.

The settlement of railway trackbed is non-linear [35], and thus changes in TQI are also often non-linear. Thus, to analyse changes in different settlement and TQI requires a numerical model that is capable of simulating daily rolling stock patterns, accounting for interactions between the different traffic types that operate in the railway infrastructure. For example, if a solely passenger line was upgraded to carry multiple freight train movements, the track resulting geometry would likely be different depending upon whether these freight trains were all run consecutively, or interspersed between passenger movements. Therefore, to most faithfully replicate changes in TQI, the traffic timetable should closely replicate true operation conditions, and vertical track profile should be updated after every axle passage [38].

To determine the relationship between TQI and tamping frequency, and thus economic cost, marginal cost analysis [39] is a useful tool. It is an important area academically and in practice given the vertical separation between infrastructure management and train operations, requiring track access charges to be set. For example, EU legislation (Directive 2012/34/EU, and the European Commission's Implementing Regulation EU 2015/909) stipulates that those charges should be based on direct costs of a train service, which can contribute to an efficient use of the infrastructure.

To address the above issues, this paper uses an engineering-economic approach to calculate marginal costs considering the evolution of railway track geometry. To do so, first a novel numerical algorithm is presented to compute differential track settlement. It uses an equivalent-linear wavenumber finite element method coupled with empirical settlement relationships in a manner that allows for the track irregularities to evolve after every load passage, before applying the next load. Compared to some traditional approaches this allows the model to faithfully simulate mixed traffic conditions, and the coupled interactions between different rolling stock types and track geometry. The model is used to calculate marginal costs of two scenarios: 1) increasing the linespeed on a passenger line, and 2) increasing the number of passenger or freight movements on a predominantly passenger line.

Engineering-economic modelling

Model architecture

A combination of engineering and economic modelling is used to predict tamping intervals and marginal costs as outlined in Fig. 1. To do so, first the engineering model is used to calculate tamping frequencies, which are then passed to the economic model which computes the related marginal costs. The engineering model is divided into two coupled steps: Step A, pre-calculation and Step B, iterative process, solved across both frequency-wavenumber and time–space domains. Step B updates the track geometry profile after every train passage, considering the evolution of deviatoric stresses in the track and ground, thus allowing for the simulation of bespoke train timetables that accommodate both passenger and freight traffic. Therefore it is capable of simulating changes to linespeed and passenger-freight traffic ratios. Based on an initial track geometry profile and a threshold intervention limit, the time-to-maintenance is calculated, as an input for marginal cost calculation.

Engineering model

Track and settlement model

The engineering sub-model uses a FEM-PML approach developed in Matlab, where the 3D stress fields are coupled with empirical settlement laws to estimate track settlement and, subsequently, future tamping intervals. The model is solved in a hybrid manner across frequency-wavenumber and time–space domains. This approach makes it well-suited for modelling repeated dynamic loads, because the track geometry profile can be updated after every axle passage with minimal computational effort. This is particularly important for operational scenarios where different types of rolling stock are operated in sequence on a daily timetable.

As shown in Fig. 1, Step A is a pre-calculation step which involves computing the 3D elastodynamic response and the geo-static stresses in the track and ground. The moving load transfer function considering non-linear track-ground stiffness is computed in the frequency-wavenumber domain. An equivalent linear approach is used to assess non-linear behaviour in the track and the ground in the frequency domain [40–43]. The effective octahedral shear strain is used to update the properties of each track-ground element until reaching convergence between the material properties and strain-adjusted properties. This non-linear calculation is performed during Step A and the strain-adjusted material properties are passed to Step B for settlement calculation. For low/medium track geometry SD's, the total stress field is dominated by quasi-static stresses, meaning the majority of non-linearity can be assumed to occur in Step A. The moving load transfer functions are then used to calculate the 3D stress transfer functions due to quasi-static and dynamic loading. Several matrices required for computing the train-track dynamic interaction are also prepared in advance. Step A is only computed once for each moving speed of vehicle and track design being considered. All variables from this part can be pre-calculated and used repeatedly in Step B.

In Step B, an iterative solver is implemented using a combination of wavenumber-frequency and space–time domains. Based on the track irregularity profile, track compliance and rolling stock, the train-track dynamic interaction force is calculated using a multi-body model. Considering the stress field in 3D, the quasi-static, geostatic, and dynamic stresses are all calculated at the track centreline and used to compute the deviatoric stress. The total deviatoric stress (combined quasi-static, dynamic and geo-static) is then used to calculate settlements in the track and the ground over the entire model track length (typically ≈200 m), in the direction of train passage. The vertical track geometry profile is updated after every axle passage and thus the train-track dynamic force and deviatoric stress are also recalculated at each iteration. These steps are repeated until a threshold limit value is reached, based upon the SD of the vertical rail profile, as commonly defined in standards. It should be noted that due to the pre-calculations performed in Step A, each Step B iteration requires minimal computational effort, thus allowing for the rapid simulation of many axle passages. To repeatedly update the track profile and account for the

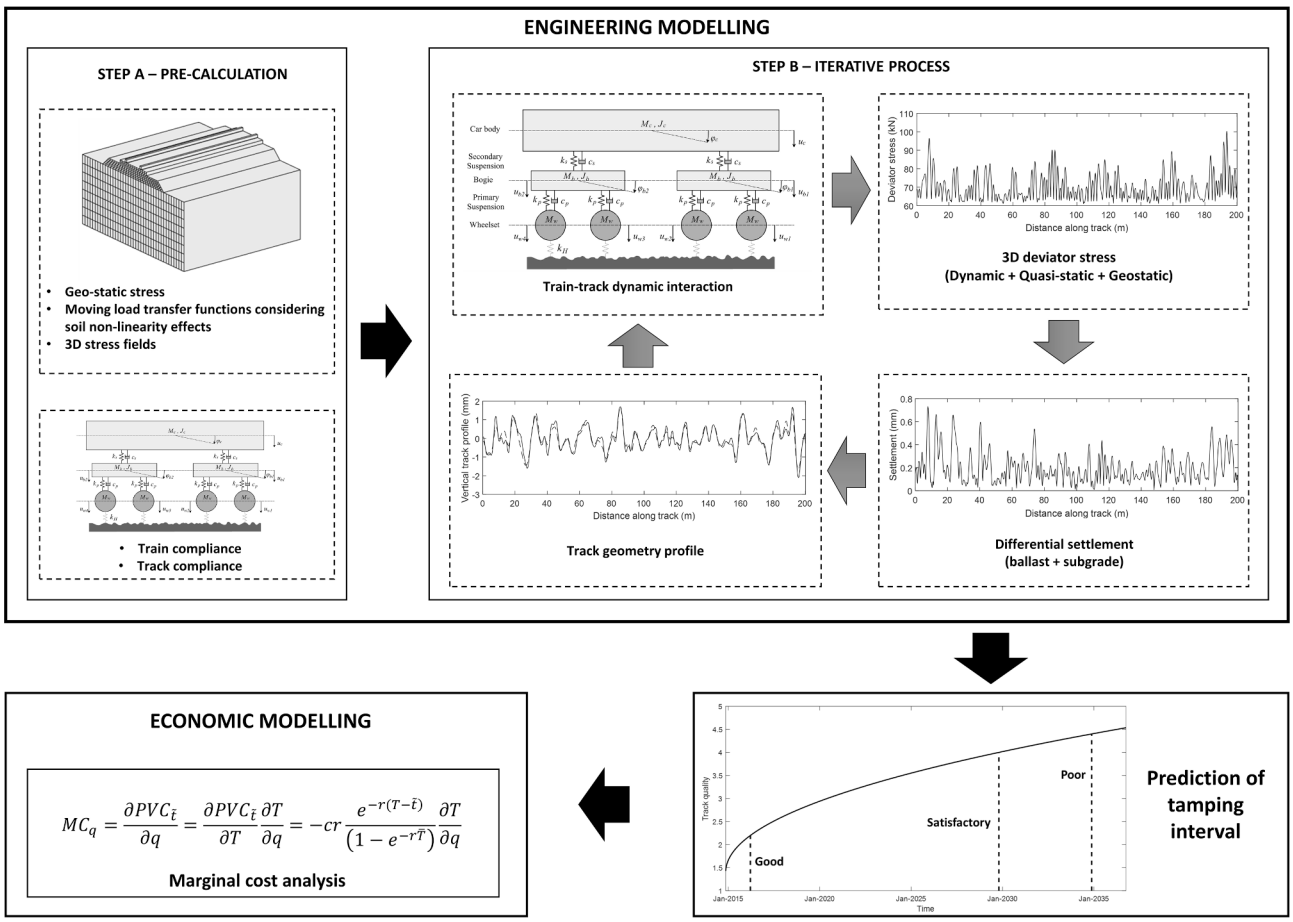

Fig. 1. Engineering-economic model overview.

settlement of previous axle passages, an incremental form of settlement equation is required. Therefore the ballast [25] and subgrade [17] settlements are calculated using Eqs. (1) and (2). Additional information regarding the empirical settlement laws can be found in [38].

$$\Delta\varepsilon_{p\_b,i} = 0.375\left(\sigma_{d\_b,i}\right)^2 \times \left[\left(1 + 0.4log_{10}\left((dN{\cdot}i) + N_{lb}\right)\right) - \left(1 + 0.4log_{10}\left((dN{\cdot}(i-1)) + N_{lb}\right)\right)\right] \quad (1)$$

$$\Delta\varepsilon_{p\_s,i} = \frac{a}{100}\left(\frac{\sigma_{d\_s,i}}{\sigma_s}\right)^m \left[\left((dN{\cdot}i) + N_{ls}\right)^b - \left((dN{\cdot}(i-1)) + N_{ls}\right)^b\right] \quad (2)$$

where $\Delta\varepsilon_{p\_b,i}$ is ballast permanent strain increment; $\Delta\varepsilon_{p\_s,i}$ is subgrade permanent strain increment; i is iterative step; $\sigma_{d\_b,i}$ is ballast dynamic deviatoric stress relevant to traffic load (in MPa); $\sigma_{d\_s,i}$ is subgrade dynamic deviatoric stress relevant to traffic load (in Pa); σ_s is soil compressive strength (in Pa); a, m, and b are material parameters; N_{lb} is the number of load cycles after the last ballast renewal/tamping; N_{ls} is the number of load cycles after the last subgrade replacement; and dN is the frequency of load application. Note that Eqs. (1) and (2) can be used for single or mixed traffic scenarios. The deviatoric stresses are computed for any arbitrary vehicle and then used to update the settlement after each cycle, considering the previous iteration. Therefore they are compatible with an arbitrary combination of traffic.

Train-track dynamic interaction model

To simulate railway vehicle dynamics, a variety of vehicle modelling approaches, each with different levels of complexity have been proposed in the literature [44], often with the goal of minimising computational requirements for their application. This goal is particularly relevant when simulating large numbers of axle passages for the purpose of differential settlement analysis. Therefore to investigate the validity of simplifying rolling stock models for the purpose of settlement calculations, a variety of common simplifications are compared. Three approaches for passenger vehicle modelling are analysed, followed by two approaches for freight. Their dynamic responses are compared because this is dominant in differential track settlement.

Firstly, to simulate the interaction between the vehicle and the track, a compliance procedure formulated in a moving frame of reference, subjected to a moving train is used [45,46]. Three common simplifications for modelling a passenger train are illustrated in Fig. 2. The first option, as shown in Fig. 2(a), is a complete vehicle model which takes into account the main structural aspects of the train dynamics. In contrast, Fig. 2(b) ignores the car box, instead only considering the dynamic motion of the bogies (semi-sprung masses) and the wheelsets (unsprung masses). Further, Fig. 2(c) only considers the presence of the wheelsets (unsprung masses) for dynamic computation.

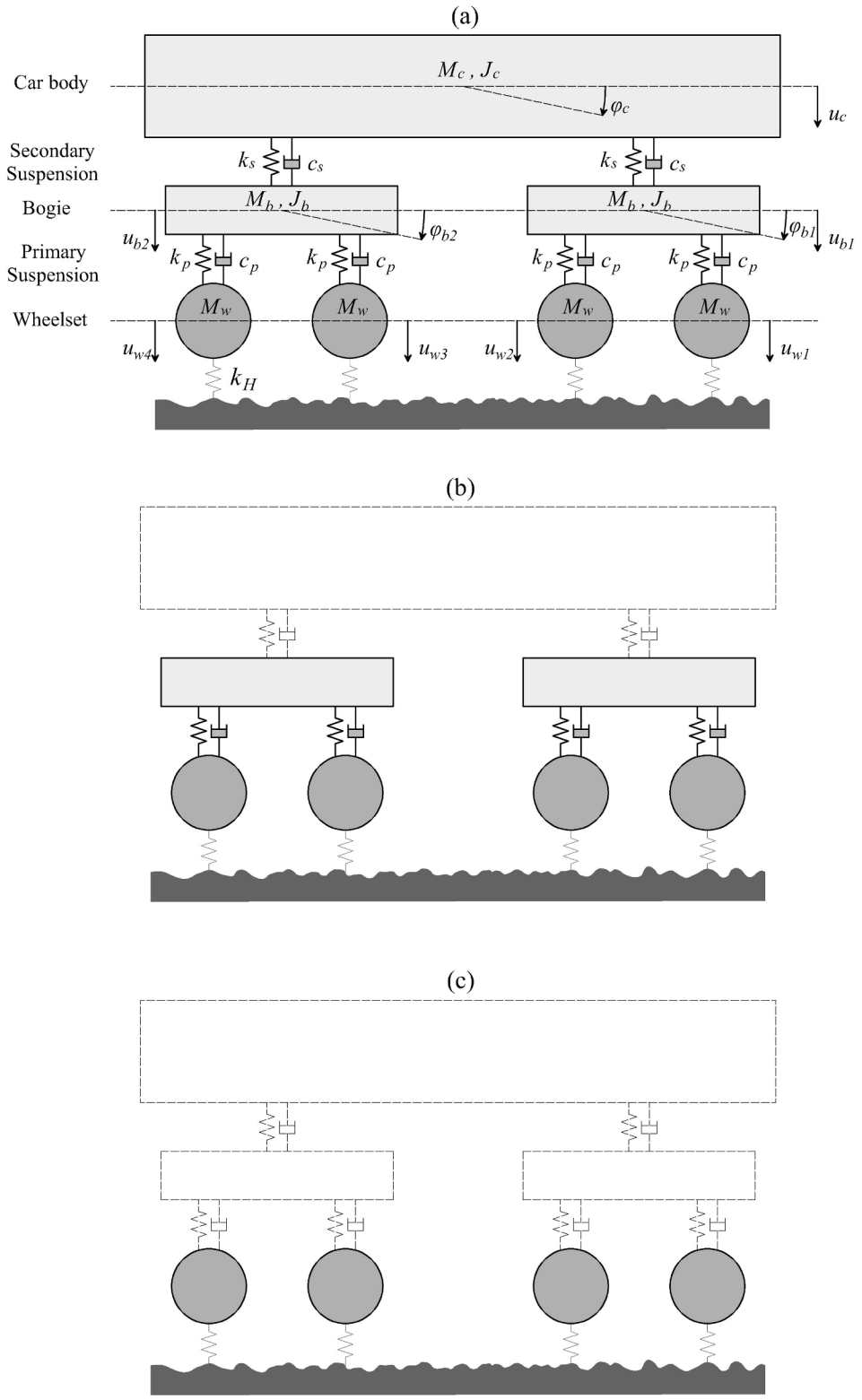

Fig. 2. Passenger vehicle modelling approaches: (a) complete vehicle model, (b) simplified model containing bogies and wheelsets, (c) simplified model containing only wheelsets.

Freight vehicles typically contain only one level of suspension, meaning only two modelling options are considered. The first option shown in Fig. 3(a) is a complete vehicle model with one level of suspension. The simplified option shown in Fig. 3(b) is where only the bogies and the wheelsets are considered.

The formulation of the dynamic interaction force in the frequency domain is:

$$\{F_{dyn}(\Omega)\} = -\left([V_c] + [V^H] + [T_c]\right)^{-1}\{\Delta u(\Omega)\} \tag{3}$$

where $\Delta u(\Omega)$ = the vertical track irregularity; T_c is the flexibility the track compliance; V_c is the flexibility of the vehicle compliance; and V^H

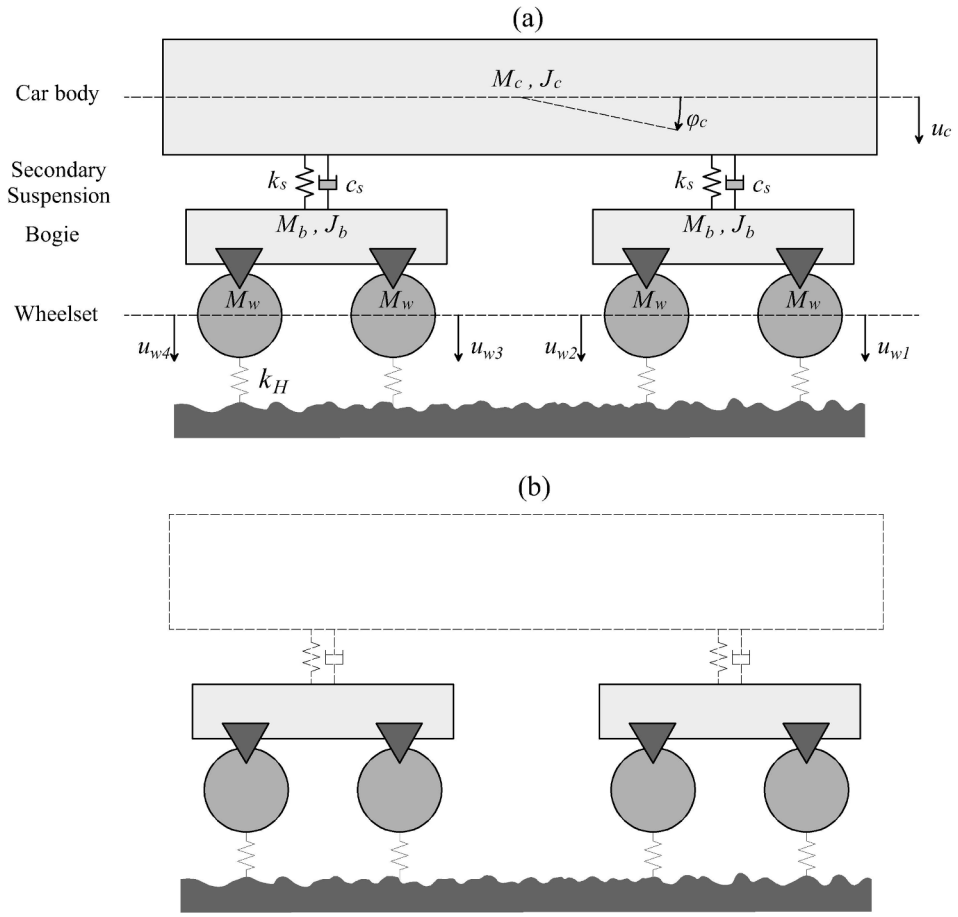

Fig. 3. Freight vehicle modelling approaches: (a) complete vehicle model, (b) simplified model of bogies and wheelsets.

Table 1
Parameters of passenger and freight vehicles.

Parameter	Passenger	Freight
Number of cars	11	40
Number of axles	44	160
Axle spacing (m)	2.9	1.7
Bogie spacing (m)	19	9.7
Car body mass (kg)	329×10^2	864×10^2
Car body pitching moment of inertia (kg.m^2)	208×10^4	102×10^4
Bogie mass (kg)	4932	2800
Wheelset mass (kg)	1538	2000
Bogie pitching moment of inertia (kg.m^2)	5150	2020
Primary suspension stiffness (kNm^{-1})	3420	–
Primary suspension viscous damping (Nsm^{-1})	360×10^2	–
Secondary suspension stiffness (kNm^{-1})	1320	2660
Secondary suspension viscous damping (Nsm^{-1})	360×10^2	25×10^2

is the contact flexibility. The details of the track compliance and the vehicle compliance, including the mass and stiffness matrices of both passenger and freight vehicles are given in Appendix A.

A simplified 2D model based on beam on elastic foundation theory [47] is used to calculate the response due to train-track dynamic interaction. An infinite Euler-Bernoulli beam is used to represent the rail which is supported by a single continuous elastic layer. It has the following material properties (single rail): Young's modulus $E = 2.1 \times 10^{11}\, N/m^2$; second moment of area $I = 30.55 \times 10^{-6}\, m^4$; cross section area $A = 0.00763\, m^2$; density $\rho = 7850\, kg/m^3$; and support stiffness $s = 100 \times 10^6\, N/m^2$. An artificial track irregularity profile for wavelengths in the range $3 < \lambda \leq 35\, m$ is generated using the PSD (Power Spectral Density) function defined by FRA [48] but the constants modified to generate specific SD profiles at higher speeds (>177 km/h).

The properties of passenger and freight vehicles are summarised in Table 1, where the properties of passenger vehicle are taken from [49] and freight vehicle adapted from [50]. The speeds of passenger and freight vehicles are 200 and 97 km/h respectively.

Fig. 4 compares the peak displacements due to dynamic loading along the track length, for the complete vehicle and simplified vehicle models. As shown in Fig. 4(a), the displacements due to the different vehicle assumptions show significant differences, however are in a similar range in terms of magnitude. In contrast, the freight vehicle shows a large discrepancy in magnitude, comparing the full and simplified vehicles - Fig. 4(b). This large difference is justified by the higher stiffness of the primary suspension and suspensions. Considering the errors associated with using simplified passenger and freight vehicles, for the purpose of differential settlement modelling, this shows it is important to use full vehicle models (i.e. avoid reducing the number of degrees of freedom).

Quasi-static versus dynamic excitation

Rolling stock moving at constant speed on plain line induces both quasi-static and dynamic excitation. The track's quasi-static deflections, stresses and strains are not influenced by track irregularities meaning they move uniformly with the load [13]. Considering the well established relationships between stress and settlement, such loading therefore also induces uniform settlement along the track. In contrast, dynamic excitation is influenced by track irregularities and is thus the source of differential settlement evolution.

To illustrate this concept more clearly, Fig. 5 shows the quasi-static and dynamic deviatoric stresses measured on the track centreline, 0.1 m below the sleeper, for an entire 200 m track length. Excitation is from the full freight train model interacting with a track irregularity of FRA's

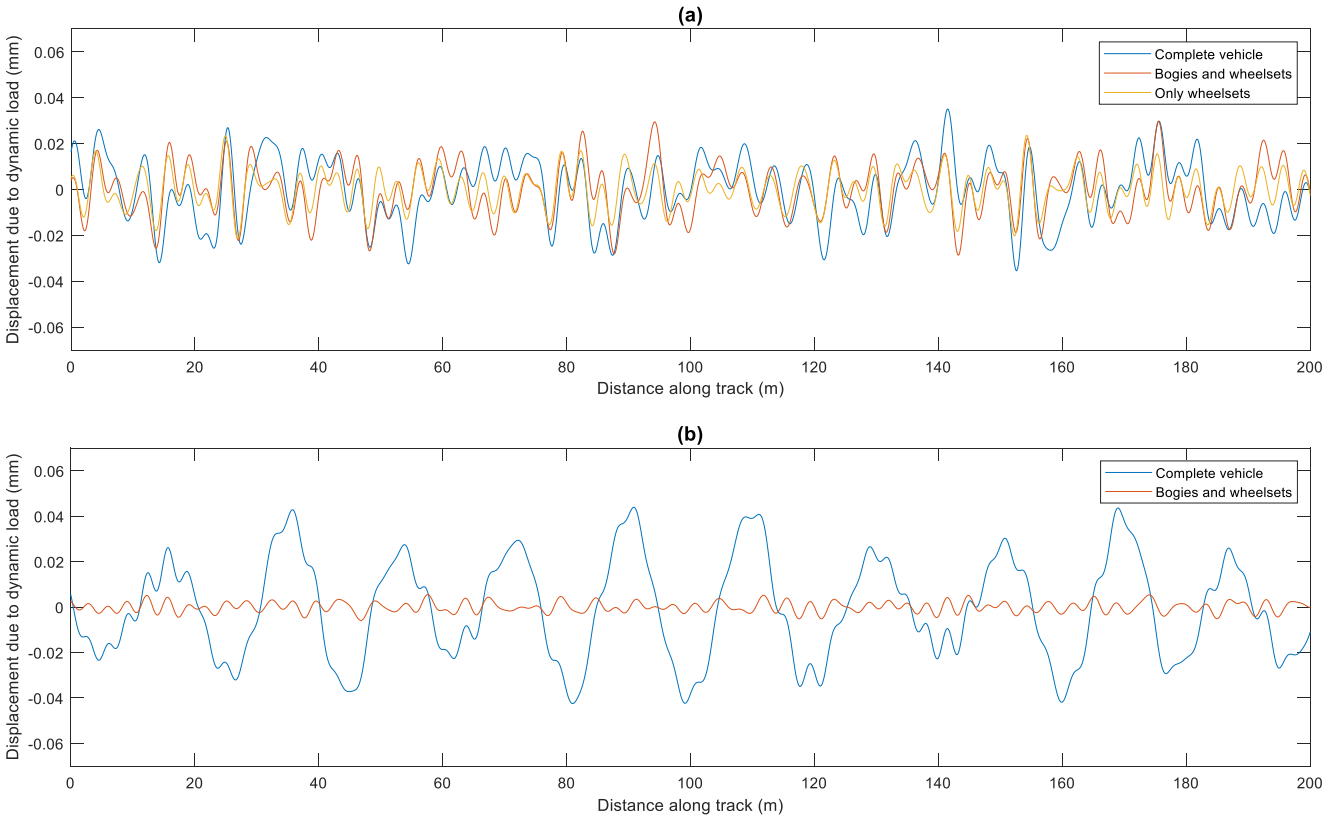

Fig. 4. Maximum rail deflection along track (dynamic excitation only): (a) passenger vehicle models (b) freight vehicle models.

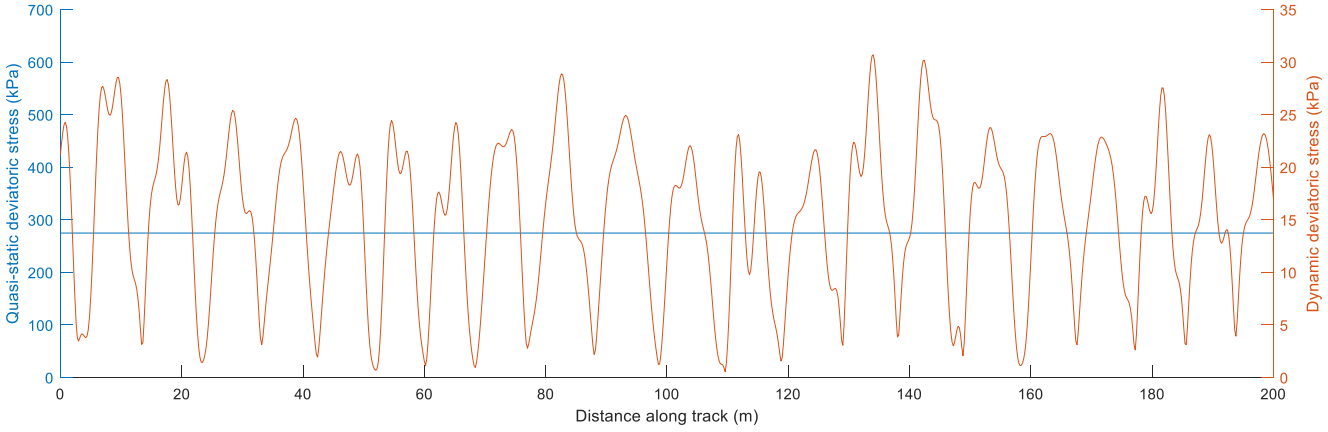

Fig. 5. Track-bed deviatoric stress due to quasi-static and dynamic excitation.

class 4 (suitable for maximum speed at 130 km/h). The corresponding ballast settlement is shown in Fig. 6. It is seen that the quasi-static excitation induces uniform settlement along the track, whereas the dynamic excitation induces non-uniform settlement along the track. This illustrates the concept that dynamic excitation is the primary driver of differential railway track settlement.

Differential settlement model validation

The ability of the model to predict the evolution of differential settlement with increasing axle passages is validated by comparing against historical track geometry data from a UK track section. The standard deviation of vertical track geometry profile over a 200 m track length is analysed, considering wavelengths in the 3–35 m range.

Fig. 7 shows the finite element mesh and dimensions of the track cross-section. The material properties of the rails, rail pads, sleepers, ballast, sub-ballast and subgrade are described in Appendix B. The subgrade properties are based upon site investigation data. The line operates almost exclusively with passenger rolling stock, and thus the vehicle properties are solely based upon the passenger vehicle shown in Table 2. The traffic volume per year is 19.58 million gross tonnes (MGT) with an operational line speed of 125mph. To facilitate validation, track geometry obtained via a Track Recording Vehicle (TRV/TRC) on 5 dates: 10-November-2014, 23-March-2015, 07-March-2016, 20-March-2017

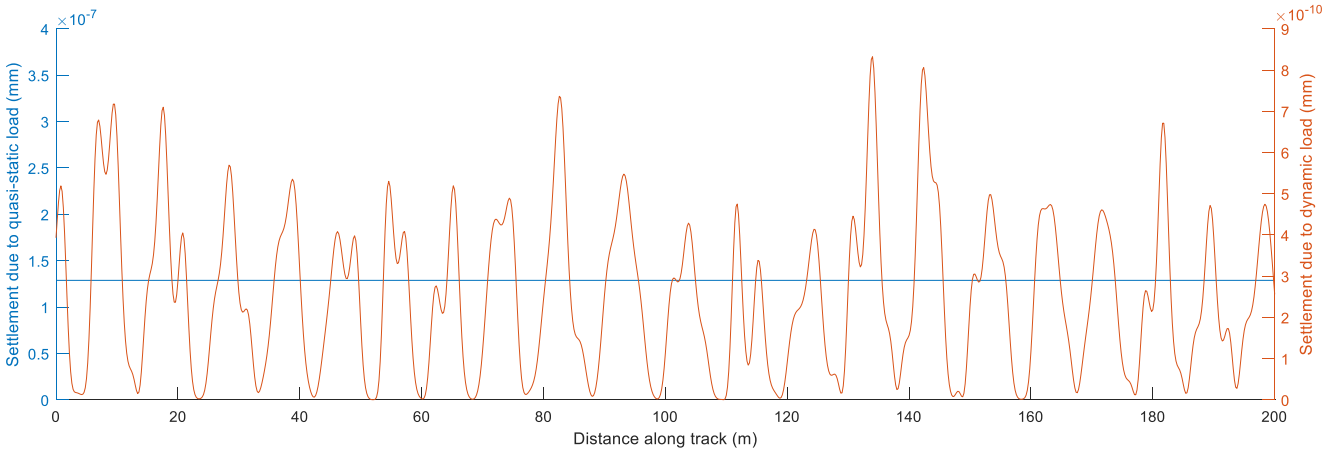

Fig. 6. Track-bed settlement due to a single axle passage. Quasi-static and dynamic components.

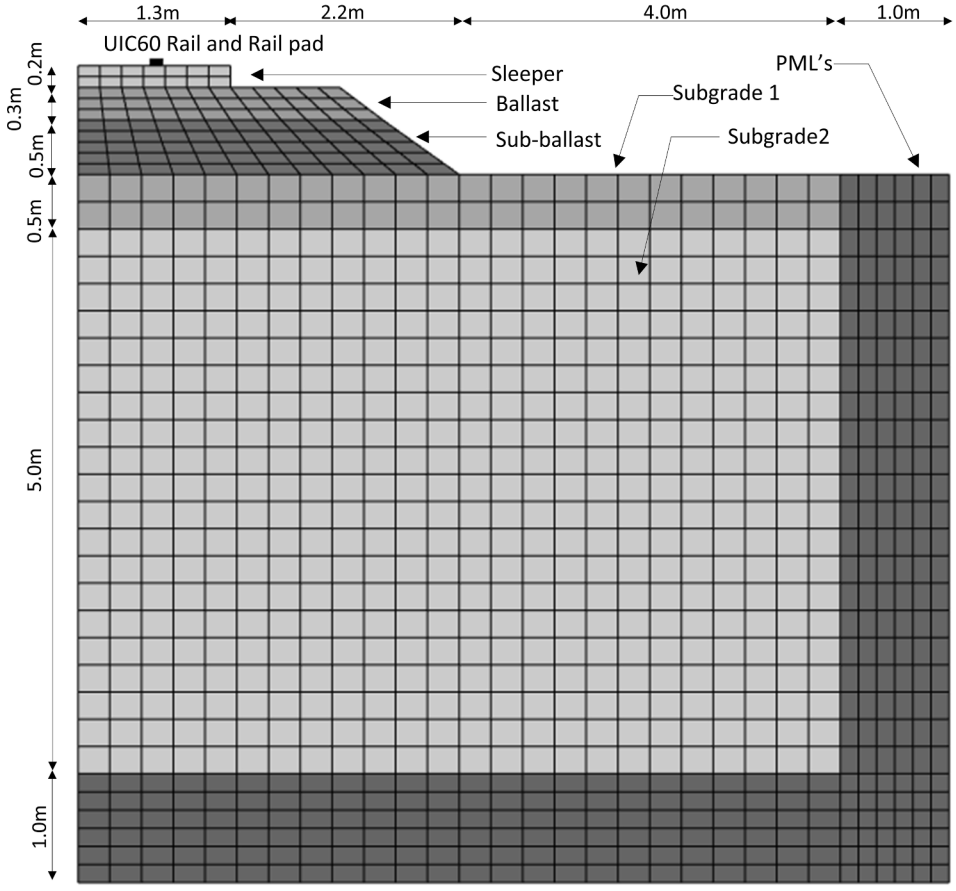

Fig. 7. Finite element mesh of the track model for validation.

and 19-March-2018, is used. Analysis of maintenance records shows that tamping was not performed between any of these dates.

The geometry data recorded on 10-Nov-2014 is used as the track starting condition. Then the model individually simulates every axle load passage until 19-March-2018. The geometry SD evolution is compared against the TRV data, as shown in Fig. 8. The rectangular markers represent the geometry SD data recorded in-situ, and the triangle marker is the SD of the initial 2014 track profile. The dashed line represents the predicted geometry SD, evolving after every axle passage. The strong correlation between the predicted geometry SD curve and the real data confirm the model is capable of predicting the evolution of differential track settlement.

Economic model

The engineering model provides the inputs for the economic model. The generalised, coupled modelling approach for direct cost calculation is:

(a) Simulate the damage from increasing the linespeed or running more trains using the engineering model
(b) Determine the timeframe until damage correction is required

Table 2
Ballast, sub-ballast and subgrade properties (case studies).

Component	Parameter	Value
Ballast	Height (m)	0.3
	Length in transversal direction (m)	2.8
	Young's modulus (Pa)	180×10^6
	Density (kg/m^3)	1650
	Poisson's ratio	0.27
	Hysteric damping coefficient	0.06
Sub-ballast (Sand-gravel)	Height (m)	0.5
	Length in transversal direction (m)	3.5
	Young's modulus (Pa)	180×10^6
	Density (kg/m^3)	2300
	Poisson's ratio	0.3
	Hysteric damping coefficient	0.05
	Settlement parameter a	0.52
	Settlement parameter b	0.15
	Settlement parameter m	1.49
	Compressive strength (kPa)	350
Subgrade (Lean clay)	Young's modulus (Pa)	70×10^6
	Density (kg/m^3)	1900
	Poisson's ratio	0.35
	Hysteric damping coefficient	0.03
	Shear wave speed (mph)	260
	Settlement parameter a	1.10
	Settlement parameter b	0.16
	Settlement parameter m	2.0
	Compressive strength (kPa)	250

(c) Calculate a unit cost of damage correction to give additional cost of increased linespeed or extra traffic on the network

The cost calculations only consider changes in tamping intervals and do not include investments in the capability of the line, i.e. fixed inputs in the production of infrastructure services. The calculated costs therefore comprise short-run marginal costs rather than long-run marginal costs. This makes the estimates consistent with the concept of direct costs for the purposes of setting track access charges.

Assuming tamping is the primary form of maintenance used to improve the SD of track, the present value cost (PVC) of an infinite time series of tamping activities at time T with constant intervals $\bar{T}$ is:

$$\lim_{n\to\infty} PVC = c\frac{1}{(1-e^{-r\bar{T}})} \tag{4}$$

where c is the tamping cost per track kilometre, and r is the annual discount rate.

Following the marginal cost calculation for track renewals in [51], a track section that is observed at time $\tilde{t}$ is considered, which is before the first tamping activity at T. The time until the next tamping activity is thus $T-\tilde{t}$. The PVC of the track section analysed in time $\tilde{t}$ is:

$$PVC_{\tilde{t}} = ce^{-r(T-\tilde{t})}\frac{1}{(1-e^{-r\bar{T}})} \tag{5}$$

To calculate a marginal cost of additional train movements, a temporary increase in tonnes Δq at time $\tilde{t}=0$ is considered, which will make the first tamping interval shorter, and all the subsequent intervals will be scheduled earlier. The subsequent intervals will have the same length as before since the traffic increase is temporary, i.e. the calculation considers the effect of one extra traffic unit running on the line. This is illustrated in Fig. 9 where T_1 is the first tamping time for the baseline case (no change to traffic), $T_1+\bar{T}$ is the second interval etc., whilst T_2 and $T_2+\bar{T}$ are the corresponding intervals for the scenario where traffic (temporarily) increases. The tamping activities are typically determined by a track geometry SD limit, as shown in Fig. 9. Note that railway administrations may also monitor the rate of change of track geometry SD and intervene if it increases suddenly, rather than only focusing on a limit value. This type of increase is more ad-hoc and can be associated with a variety of alternative deterioration mechanisms, including shrink-swelling of clay embankments. Therefore this paper focuses upon planned interventions.

The marginal cost is expressed as:

$$MC_q = \frac{\partial PVC_{\tilde{t}}}{\partial q} = \frac{\partial PVC_{\tilde{t}}}{\partial T}\frac{\partial T}{\partial q} = -cr\frac{e^{-r(T-\tilde{t})}}{(1-e^{-r\bar{T}})}\frac{\partial T}{\partial q} \tag{6}$$

In this calculation, an increase in traffic during the first tamping interval is considered which can be expressed as the change in the average annual tonnes, $\frac{\partial \bar{q}_1}{\partial q}$. As noted by [51,52], this change can be

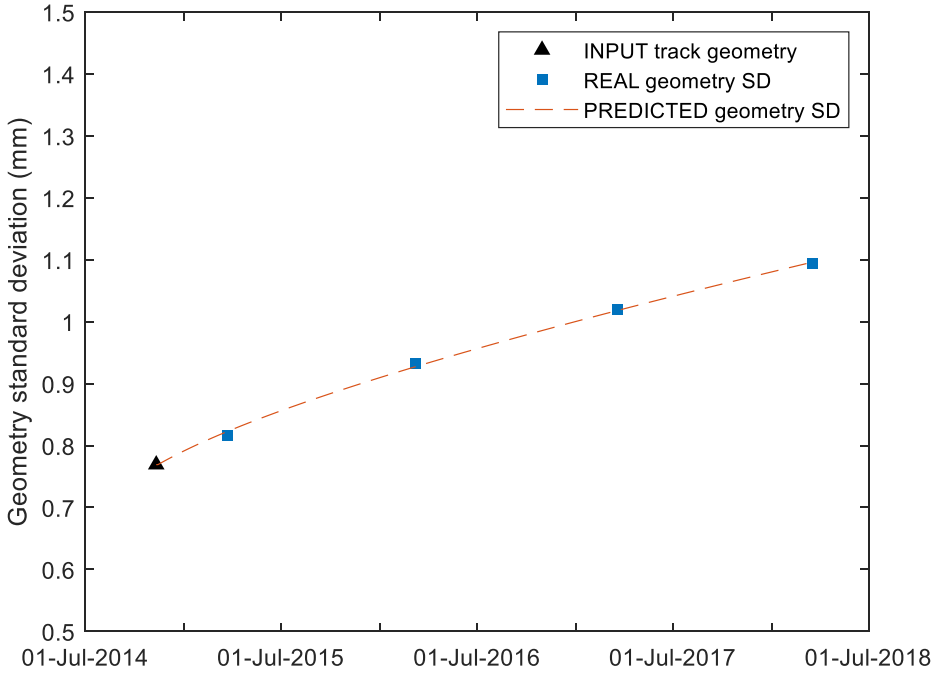

Fig. 8. Validation of vertical rail profile SD over time: predicted vs field data.

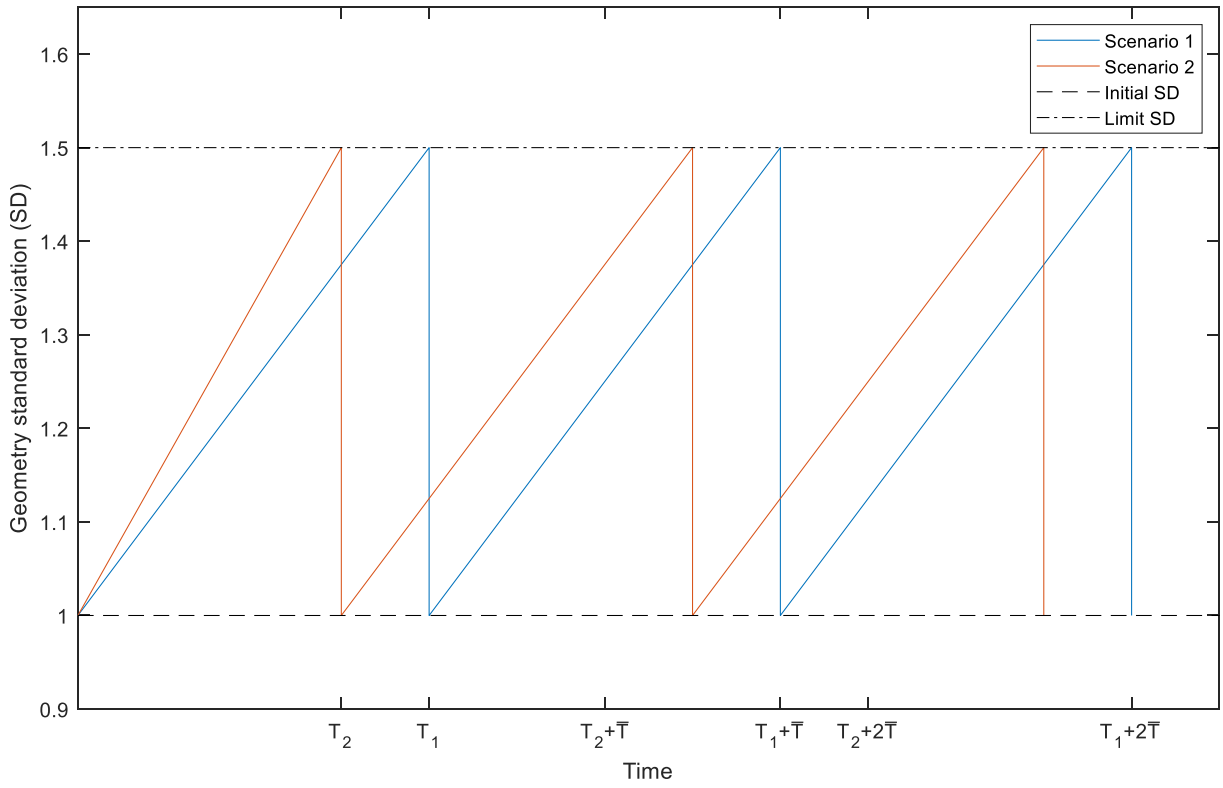

Fig. 9. Idealised tamping interval concept for two scenarios.

approximated as $\frac{\partial \bar{q}_1}{\partial q} \approx \frac{1}{T}$, which has a decreasing error the more stable the traffic volume is. That is, the change in tamping interval due to a (percentage) change in tonnes is:

$$\frac{\partial T}{\partial q} = \frac{\partial T}{\partial \bar{q}_1}\frac{\partial \bar{q}_1}{\partial q} = \frac{\partial T}{\partial \bar{q}_1}\frac{1}{T} \tag{7}$$

This is expressed in terms of a deterioration elasticity, $\gamma_q = \frac{\partial T}{\partial \bar{q}_1}\frac{\bar{q}_1}{T}$. The marginal cost in Eq. *(4)* is expressed as:

$$MC_q = \frac{\partial PVC_{\tilde{t}}}{\partial q} = -cr\frac{e^{-r(\tilde{T}-\tilde{t})}}{(1-e^{-r\tilde{T}})}\frac{\gamma_q}{\bar{q}_1} \tag{8}$$

Note that c is cost per track-km, which is multiplied by one over tonnage ($\frac{1}{\bar{q}_1}$), and the marginal cost is thus a cost per tonne per track-km, i.e. cost per tonne-km.

The marginal cost calculation for a temporary change in the speed (v) for traffic is like the calculation for an increase in tonnage. The deterioration elasticity γ_v is the percentage change in tamping interval after a percentage change in speed, and $\bar{v}_1$ is the annual speed during the first tamping interval. This marginal cost calculation also uses cost per track-km (c), which is multiplied by one over speed ($\frac{1}{\bar{v}_1}$) and the marginal cost is thus expressed as a cost per v per track-km (i.e. cost per v-km). In other words, it is the extra cost per v (km/h) for a train running on one km of track.

$$MC_v = \frac{\partial PVC_{\tilde{t}}}{\partial v} = \frac{\partial PVC_{\tilde{t}}}{\partial T}\frac{\partial T}{\partial v} = -cr\frac{e^{-r\left(\tilde{T}-\tilde{t}\right)}}{(1-e^{-r\tilde{T}})}\frac{\partial T}{\partial v} = -cr\frac{e^{-r(\tilde{T}-\tilde{t})}}{(1-e^{-r\tilde{T}})}\frac{\gamma_v}{\bar{v}_1} \tag{9}$$

Case studies

The validated model is used to perform two analyses. Firstly it is used to analyse the effect of increasing line speed on differential track settlement, comparing speeds of 201, 209, 217 and 225 km/h (125, 130, 135 and 140mph). Secondly, it is used to investigate the effect of adding additional passenger or freight trains on the settlement of an existing track.

Track parameters

The finite element track mesh is the same as Fig. 7, however to reduce the number of potentially influential variables, the thin upper soil layer is assigned the material properties of the supporting soil layer below it. The track parameters including the characteristics of the rails, rail pads and sleepers are the same as the validation case, and are shown in Appendix B. The properties of ballast, sub-ballast and subgrade are summarised in Table 2. Considering the two applications under investigation (linespeed and additional trains), the only track difference is the vertical geometry track profile.

Operational parameters

The operational parameters are kept similar to the validation case, with a traffic volume per year of 19.58 million gross tons (MGT), and an average traffic volume per day of 0.054 MGT. The traffic volume is converted to passenger trains assuming an 11-car train with 17 tonne axle loads.

$$\text{Number of trains per MGT} = \frac{10^6}{(44*17)} \approx 1337 \text{ trains}$$

The MGT per passenger train is thus approximately $\left(\frac{1}{1337} \approx\right)$ 0.00075. For freight trains, the calculation is based on a 50-car train with 25 tonne axle weights.

$$\text{Number of trains per MGT} = \frac{10^6}{(160*25)} \approx 250 \text{ trains}$$

The MGT per freight train is thus $\left(\frac{1}{250} =\right)$ 0.004.

Tamping costs

A tamping cost per track-km is required to calculate a marginal cost. It is assumed tamping is performed using machines with an output of 400 m/h, and a mean cost per shift of £9k. The on-site working time is approximated as 3–4 h (e.g. 07/08 Plasser or equivalent Matisa machines), however it is recognised that productive time is highly variable, due to the many factors that influence transit from the stabling point to site and return. This means approximately 1.6 track-km can be tamped during a shift. The tamping cost per track-km is then £5,625. The engineering simulations cover 200 m lengths of track, however it is assumed the machine and shift will do a longer section, and calculate

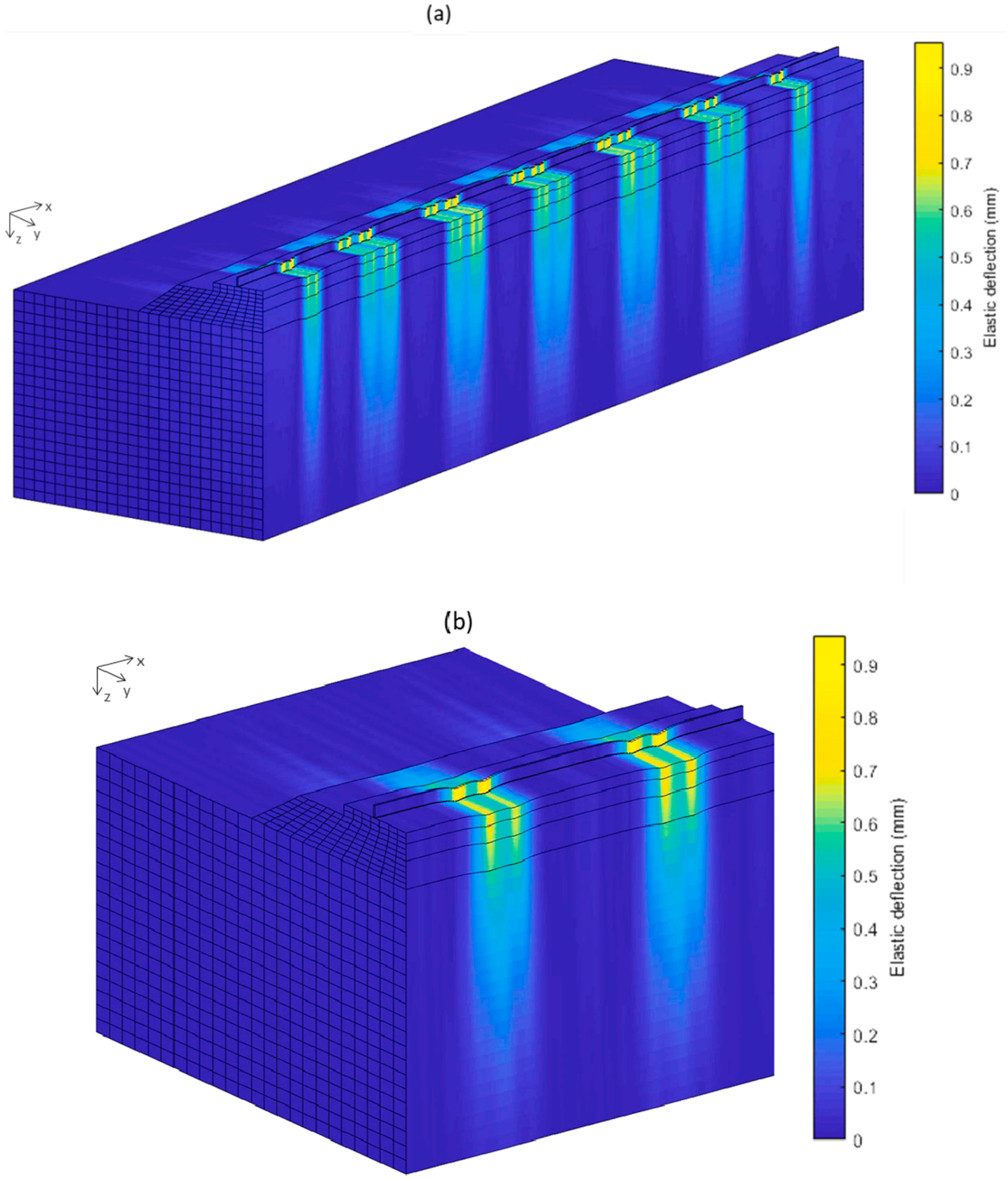

Fig. 10. 3D track-ground deflection profile (slice along track centreline considering both quasi-static and dynamic excitation): (a) a full vehicle over a 200 m track length with an XYZ aspect ratio of [8 1 1] (b) one car zoomed in over a 40 m track length.

costs per track-km.

Analysis and results

Engineering analysis

Two analyses are performed. First the influence of linespeed on differential track settlement is investigated, considering four linespeeds: 201, 209, 217 and 225 km/h (125, 130, 135 and 140mph). The second analysis is the influence of increased passenger and freight train movements on the settlement of a predominantly passenger-only line.

The influence of linespeed on track settlement

The profile used for the previous validation case is worse than typically allowable on a track with a linespeed of 225 km/h. Therefore a starting track geometry profile is artificially generated using the PSD function [48]. Wavelengths between 3 and 35 m are used because the aim of the model is to predict automated tamping intervals, and this range is typically associated with the faults that can be corrected via tamping. An initial track profile characterised by a SD of 1.03 mm over 200 m length is generated and it is assumed the track historically experienced 100 k cycles of passenger train axles prior to the start of the simulations. This is intended to replicate the influence the dynamic track stabilisation process commonly performed post-renewal. Then the model simulates differential settlement evolution due to traffic, to a threshold of 1.5 mm for four moving speeds: 201, 209, 217 and 225 km/h. For all speeds the track and its vertical profile remain fixed.

Fig. 10 illustrates the 3D track-ground displacement contour for the passenger train at 201 km/h and the response propagating from the rail into supporting track-ground structure. Note that for Fig. 10(a), although the domain shown is the full 200 m track section with a 158.9 m long train, to maximise viewability, the x-axis is scale is scaled by a factor of 8 compared to the y and z-axis.

Fig. 11 shows the vertical track geometry profiles for the four different speeds at the instant they reach the threshold limit. Similarly, Fig. 12 compares the evolving geometry SD over time from the initial SD value until the threshold limit. The corresponding time until threshold exceedance is summarised and compared in Table 3. The time until threshold exceeded when running passenger trains with speeds 201, 209, 217 and 225 km/h are 697, 620, 585 and 568 days respectively. These correspond to reductions of: 11 %, 16.1 %, and 18.5 %.

These reductions show linespeed increases can have an important impact on differential track settlement, and the time until threshold exceedance is significantly reduced. This is further confirmed in Fig. 13, which shows rates of SD change per year for each linespeed. The rate of SD change per year is approximately 0.244 mm for a speed 201 km/h and increases to 0.274, 0.290 and 0.299 mm when increasing line speed to 209, 217 and 225 km/h respectively. Also, Fig. 14 illustrates the moving average of SD over time, for each line speed. It should be noted

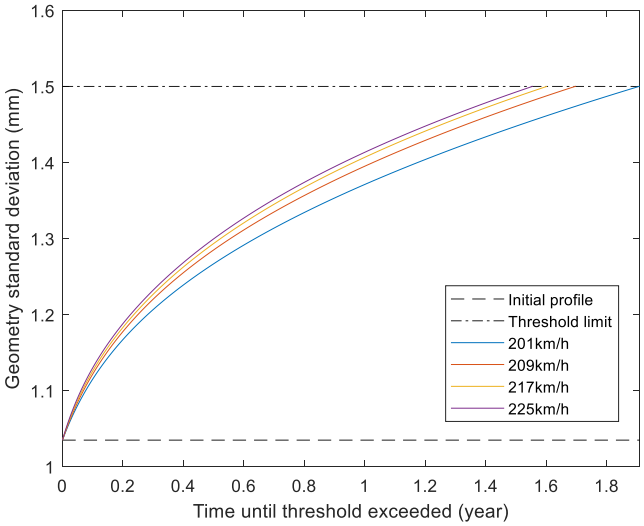

Fig. 12. Vertical rail profile standard deviation evolution over time for varying linespeeds.

Table 3
Time until threshold exceedance for varying linespeeds.

Linespeed (km/h)	Time until threshold exceeded (days)	Percentage decrease
201	697	0 %
209	620	11.0 %
217	585	16.1 %
225	568	18.5 %

that the degradation is sensitive to the rolling stock dynamics, and it is assumed that the speed of existing rolling stock would just be increased. In real life, considering the increased speed, dedicated high speed trains might be chosen, with different dynamics and wheel profiles, depending on the radius of curves on the route. Further, track improvements (e.g. under sleeper pads) might also be installed to improve the track's structural response, before increasing linespeed. These factors would influence track settlement.

To further investigate the drivers behind the growth in settlement, the deviatoric stresses due to the vehicle's quasi-static and dynamic loading components are shown in Fig. 15 and Fig. 16. Quasi-static excitation represents the rolling stock components that are not excited during vehicle-track interaction, and thus act as a constant moving force. The relevance of this excitation mechanism grows when approaching the track-ground critical velocity [12,13], but is insensitive to track irregularities. Alternatively, the dynamic excitation is related to the train-track interaction, and heavily influenced by the wheel-rail

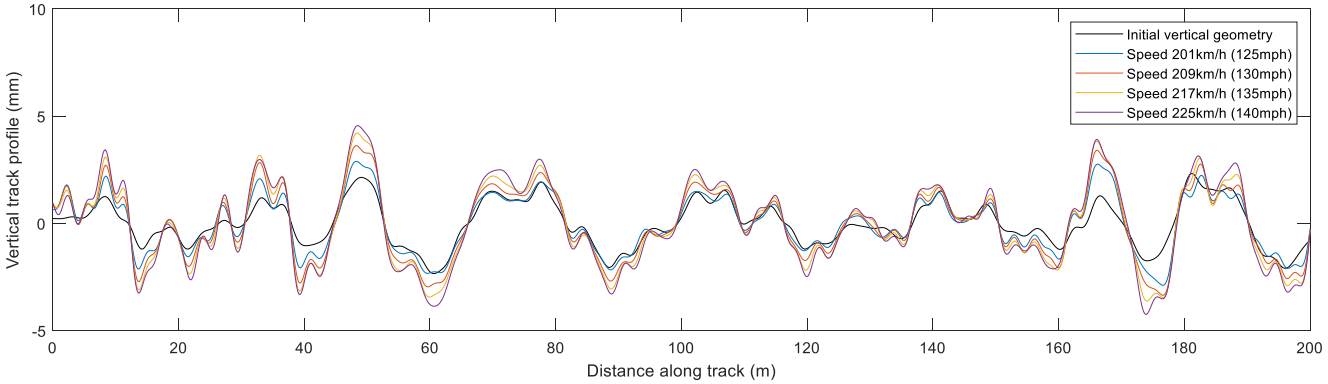

Fig. 11. Vertical track profiles after reaching the threshold limit for four train speeds (3–35 m wavelength filter).

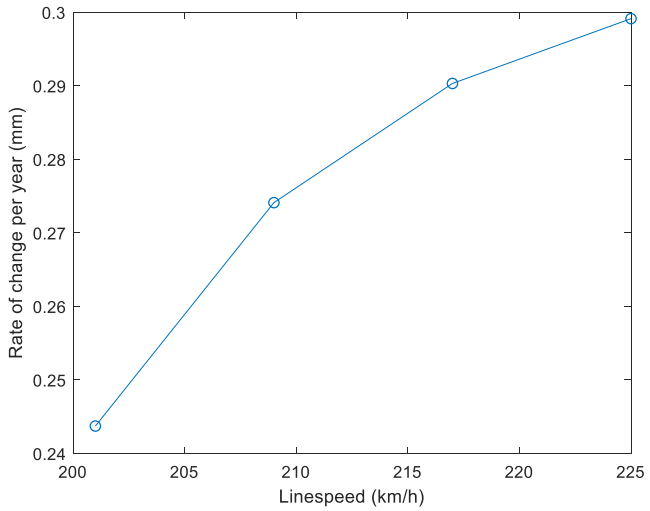

Fig. 13. Rates of average SD change per year for each line speed.

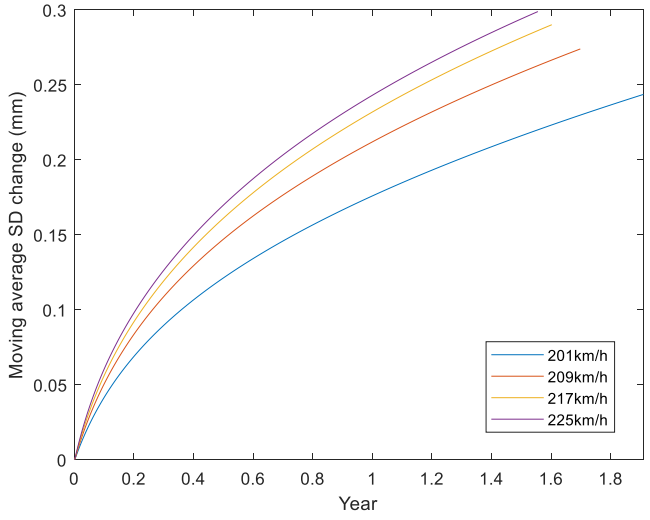

Fig. 14. Moving average SD change over time.

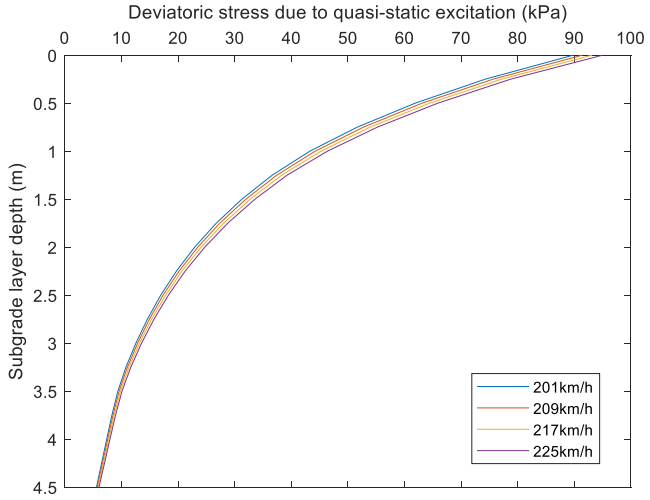

Fig. 15. Deviatoric stress vs depth, due to quasi-static vehicle excitation.

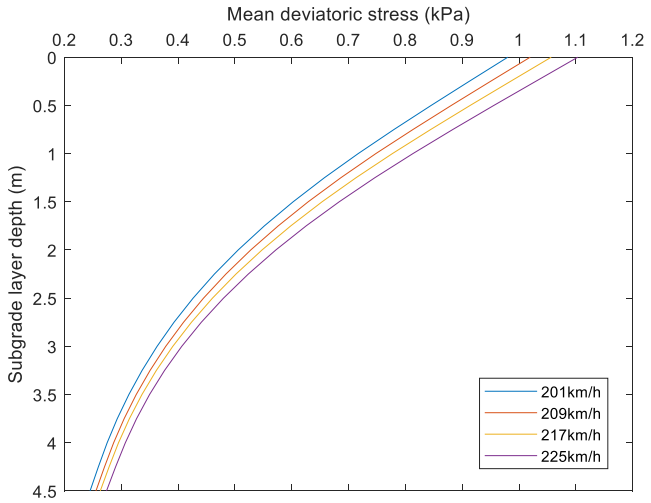

Fig. 16. Deviatoric stress vs depth, due to dynamic vehicle excitation.

Table 4
Percentage differences in deviatoric stress.

Linespeed (km/h)	Percentage difference in deviatoric stress	
	Quasi-static excitation	Dynamic excitation
201	0 %	0 %
209	1.8 %	4.1 %
217	3.7 %	7.8 %
225	5.8 %	12.7 %

Table 5
Operational mixed railway traffic scenarios.

	Scenario A	Scenario B	Scenario C	Scenario D
Passenger trains/day	72	73	72	72
Freight trains/day	0	0	1	2
Passenger MGT/day	0.054	0.05475	0.054	0.054
Freight MGT/day	0	0	0.004	0.008
Passenger MGT/year	19.58	19.5875	19.58	19.58
Freight MGT/year	0	0	1.46	2.92
Total MGT	19.58	19.5875	21.04	22.50

irregularities and vehicle suspension. Table 4 summarises the percentage differences in mean deviatoric stress measured at subgrade surface when increasing linespeed. Considering the stress field in 3D, the deviatoric stress is calculated by Eq. *(10)* which is dependent on the sum of squares of the differences of the principal stresses. It is shown that quasi-static deviatoric stresses increase by 1.8 %, 3.7 % and 5.8 %, while the dynamic deviatoric stresses increase by 4.1 %, 7.8 % and 12.7 %, when increasing linespeed to 209, 217 and 225 km/h respectively. Considering deviatoric stress is directly related to permanent deformation, the increase in dynamic excitation contributes more dominantly to the differential settlement than quasi-static.

$$\sigma_d = \sqrt{\frac{1}{2}} \times \sqrt{(\sigma_1 - \sigma_2)^2 + (\sigma_2 - \sigma_3)^2 + (\sigma_3 - \sigma_1)^2} \tag{10}$$

The influence of increased train movements on track settlement

Four traffic scenarios are simulated. Firstly, the case of 100 % passenger trains acts as the baseline case. Then, three additional scenarios are simulated to understand the effect of adding additional passenger or freight services to the baseline case: B) adding 1 passenger train, C) adding 1 freight train, and D) adding 2 freight trains. The relationship between these scenarios and annual operational tonnage is summarised in Table 5. The passenger and freight trains are operated at constant

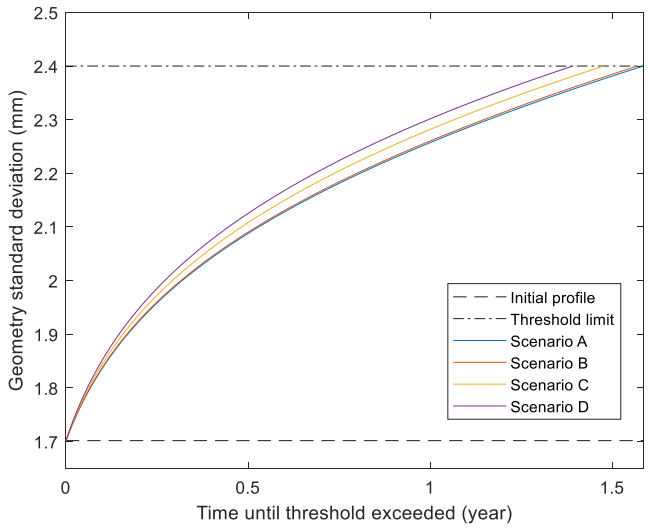

Fig. 17. Standard deviation with duration until threshold exceedance for four scenarios.

Table 6
Time until threshold exceeded for additional passenger and freight scenarios.

Traffic scenario	Percentage increase in MGT	Time until threshold exceeded (days)	Percentage decrease in time
(A) 100 % passenger trains	0 %	579	0 %
(B) Adding 1 passenger train per day	1.4 %	573	1.0 %
(C) Adding 1 freight train per day	7.4 %	539	6.9 %
(D) Adding 2 freight trains per day	14.8 %	504	13.0 %

speeds of 200 and 97 km/h respectively. For all cases, the number of passenger train movements are equal, or higher, than the baseline case. Considering the high number of passenger movements per day on the line, it's challenging to add slow-moving freight movements between individual passenger trains during the hours of peak travel. Instead, on such a line is realistic to assume that passenger services run during the day, while freight movements are confined to evenings/nights. To simulate such a scenario, the required daily number of passenger trains are run in a row, followed by the daily number of freight trains. Therefore there is interdependency between the differential settlements induced by both vehicle types.

The same track is considered as for the previous linespeed analysis. However, considering the lower maximum linespeed under consideration, and that the line experiences mixed traffic, the typical SD is likely to be higher. Therefore, assuming a maximum operational linespeed of 200 km/h, an initial track profile is artificially generated with SD = 1.7 mm, and the threshold limit is set as 2.4 mm. To keep the analysis consistent, as for the linespeed analysis, it is assumed that the track has also experienced 100 k loading cycles at the start of the numerical simulations. In reality, this number is likely to be higher unless maintenance activity is performed prior to introducing the additional traffic movements. Also note that it is assumed the track has experienced freight traffic in the past and therefore has experienced equivalent stress states. Thus, the empirical relationship between settlement and deviatoric stress is valid for both passenger and freight vehicles.

Regarding simulation results, the evolving geometry SD over time, from the initial SD value until the threshold limit value is compared in

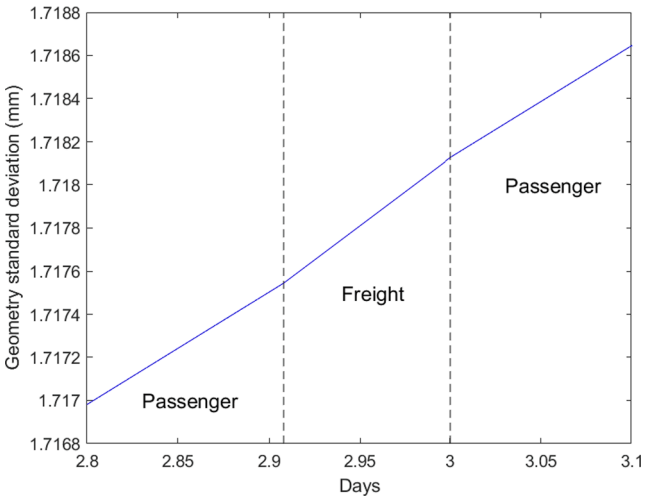

Fig. 18. Standard deviation change for scenario D.

Fig. 17, and summarised in Table 6. The durations until threshold exceedance for scenarios A, B, C and D are 579, 573, 539 and 504 days respectively. Note that the time until the threshold is exceeded in the baseline scenario A is shorter (579 days) than in the previous linespeed analysis (697 days) because a different initial track profile and threshold limit is under consideration.

It is found when adding 1 passenger train per day (1.4 % MGT) the time-to-maintenance reduces by 1.0 %. In contrast, the time reduces by 6.9 % when adding 1 freight train per day (7.4 % MGT) and 13.0 % when adding 2 daily freight trains (14.8 % MGT).

This shows the effect of additional freight traffic is more pronounced in comparison to adding additional passenger services, which is due to differing dynamic characteristics of the vehicles (Fig. 4) and also quasi-static load. This is shown in greater depth in Fig. 18 which displays the effect of traffic on SD evolution between days 2.8 and 3.1, for scenario D. The gradient of SD change is greater during the hours of freight train passage, compared to passenger.

The relationship between the effect of each scenario on MGT and the duration until threshold exceedance is also shown in Table 6. It is seen that there is a positive correlation between both, however for the additional passenger train case, compared to the freight case, the increase in maintenance relative to MGT increase is lower.

Marginal tamping cost analysis

The influence of linespeed on cost

The deterioration elasticity with respect to speed, $\gamma_v = \frac{\partial T}{\partial \bar{v}_1}\frac{\bar{v}_1}{T}$, is calculated using the percentage change in tamping intervals divided by the percentage change in km/h. The same approach is used when calculating the deterioration elasticity with respect to gross tonnes, $\gamma_q = \frac{\partial T}{\partial \bar{q}_1}\frac{\bar{q}_1}{T}$. These elasticities are negative because increased linespeed or increased gross tonnes reduces the time until the threshold for track geometry SD is exceeded. The elasticities are combined with tamping costs per track-km to calculate marginal tamping costs with respect to track settlement – see Eq. *(8)* and Eq. *(9)*. A discount rate of 3.5 % is used, as recommended in the Transport Analysis Guidance (TAG)

Table 7
Marginal cost per km/h/1000 train-km with 200 km/h as the baseline.

Scenario	Elasticity	Marginal cost, £ per km/h/1000 train-km
(A2) Increasing speed to 209 km/h	−2.78	1.445
(A3) Increasing speed to 217 km/h	−2.02	1.012
(A4) Increasing speed to 225 km/h	−1.55	0.750

published by the UK Department for Transport.

The elasticities for the different linespeed scenarios are presented in Table 7. The marginal costs are expressed as an average marginal cost per km/h/1000 train-km since the increases in speed apply to all trains running on the line, which is 26,176 passenger trains per year. Although there are limited number of studies on the effect of changing linespeed on marginal costs, as a comparison based on visual inspection of reported data points in [52] the difference in marginal cost for settlement between vehicles with speeds at 140 km/h and 200 km/h (16 tonne axle load) indicates an extra cost of SEK 224.40 per 1000 train-km in 2021 prices, and SEK 3.74 per km/h/1000 train-km. Using the conversion rate £ 1 = SEK 12, the marginal cost is £ 0.400 per km/h/1000 train-km.

Although this is similar, albeit lower than the figures shown in Table 7, there are important differences between the analyses: 1) [52] is based on changes in speed from 140 to 200 km/h, which is lower than the speeds considered in the scenarios in Table 7. This is important because higher speeds result in higher train-track dynamic effects; 2) At the lower speeds considered by [52], the SD band between threshold values is wider than for higher speeds. For example, this analysis considers a SD change of 0.5 mm (1–1.5 mm), while later in this paper for freight analysis on a lower speed line considers a SD change of 0.7 mm (1.5–2.4 mm). Therefore, at lower speeds, the threshold will take longer to meet, thus lowering marginal cost. Further, it is likely that [52] considered changes within the 3–25 m wavelength range, while this work considers 3–35 m; 3) [52] uses costs from 2001. Industry changes (e.g. improvements in health and safety and sustainability) are likely to have resulted in tamping price costs rising above the standard measure of inflation. This will manifest as higher marginal costs when considering current prices.

The influence of Rolling stock movements on cost

The elasticities and marginal costs for the different scenarios of increased train movements are presented in Table 8. This indicates that adding 1 passenger train per day has a similar influence on tamping costs as adding 2 freight trains per day, whilst the highest marginal cost is generated by adding 1 freight train per day.

These costs are lower than, but in the same order of magnitude as, the marginal costs in the econometric literature on rail infrastructure maintenance costs. For example, the marginal cost per 1000 tonne-km for track maintenance in France [53] is € 0.380 and € 0.934 for freight traffic and passenger traffic, respectively, which corresponds to £ 0.317 and £ 0.778 using the conversion rate £ 1 = € 1.20. Note, however, that these are estimates that consider all types of track damages and track maintenance activities and not only settlement and tamping. Moreover, [39] make use of a hybrid model that combines engineering and econometric methods and reports marginal costs for track settlement for different vehicle types. The average marginal cost per 1000 tonne-km for settlement is £ 0.565 for a freight train and £ 0.456 for a passenger train (based on their model with explanatory variables for RCF, wear, and settlement). These costs are also higher than the marginal costs in Table 8, but this is expected since [39] consider costs for tamping as well as all other track maintenance activities that can be triggered by settlement.

The results in Table 8 are similar to the engineering results on the marginal cost for track settlement in [52]. Based on visual inspection of an illustration with marginal costs for passenger cars, locos, and coaches, the average marginal cost per 1000 tonne-km for a passenger train (1 loco and 11 cars) is SEK 1.119 in 2021 prices which is £ 0.093 using the conversion rate £ 1 = SEK 12. These trains are running at 160 km/h and the cars have an axle load at 13 tonnes. The corresponding cost for a coach with a vehicle speed at 200 km/h (axle load 16 tonnes) is £ 0.190. The average marginal cost per 1000 tonne-km for a freight train (1 loco and 50 wagons) is £ 0.185.

Table 8
Marginal cost per 1000 tonne-km.

Scenario	Elasticity	Marginal cost, £ per 1000 tonne-km
(B) Adding 1 passenger train per day	−0.75	0.131
(C) Adding 1 freight train per day	−0.93	0.153
(D) Adding 2 freight trains per day	−0.87	0.134

Discussion

The preceding sections highlight the changes to track tamping intervals and costs when changing linespeed and adding additional tonnage. For both analyses, the initial compacted state of the ballast plays a dominant role. It is the initial cycles where settlement is most rapid, and during this period the train-induced dynamic stresses can rapidly alter the differential settlement characteristics of the track, thus exasperate changes in standard deviation. Therefore, as an example, regarding the aforementioned freight analysis, if the line was not assumed to have been recently renewed, then initial assumption of 100 k cycles would be higher, and the marginal cost would be lower.

Further, differential settlement is closely related to dynamic train-track interaction, and thus effected by rolling stock properties. For freight vehicles, in practise there are often limited details related to their payload magnitudes, load distribution across neighbouring axles/cars and sometimes even rolling stock schedule. Also, freight vehicle characteristics (e.g. suspension) can vary vastly between trains.

Regarding costs, only the cost of vertical track geometry correction is considered, while the effect of additional damage is ignored (e.g. rolling contact fatigue). Although an average cost of tamping is assumed, this is subject to variability due to a wide range of factors. For example, how close is the nearest tamper stabling point, how long is the possession, is a pre- and post-work track recording vehicle run needed…etc. Note that the marginal costs in Table 7 and Table 8 can be re-calculated with respect to alternative unit costs (£c_{new} in 2021 prices) using the multiplication factor $c_{new}/5625$, where 5625 is the unit cost (tamping cost per track kilometre) assumed in this paper.

Considering the above, it should be noted that the analysis in this paper is based upon a single set of simulation parameters, and the results are sensitive to these. When investigating the effect of speed and rolling stock characteristics in practise, it is recommended this should done on a case-by-case basis to maximise accuracy.

Conclusions

Under repeated train passages, railway tracks settle differentially due to dynamic train-track interaction. When linespeed is increased, or new rolling-stock is introduced, this can alter the rate of change of differential settlement. Therefore this paper presents a new combined engineering-economic approach to investigate the effect of increasing train speeds, adding additional passenger movements, and adding additional freight movements to an existing line. This has the advantage over traditional statistical methods because it doesn't rely on previous historical geometry data for extrapolation.

Firstly a novel numerical engineering algorithm is presented to compute differential track settlement. It uses the wavenumber finite element method coupled with empirical settlement relationships in a manner that allows for track irregularities to evolve after every load passage, before applying the next load. This allows the model to faithfully simulate mixed traffic conditions, and the coupled interactions between different rolling stock types and track geometry. The engineering model is coupled with an economic model capable of calculating marginal cost, which is useful for infrastructure managers that want to predict the tamping costs of for example higher linespeeds or additional passenger or freight train movements. This is also relevant for setting track access charges that can contribute to an efficient use of the infrastructure.

The model is validated using track recoding car data from an in-situ track and then used to investigate increasing the linespeed on a passenger line. It's shown that for an example track scenario increasing the linespeed by 25 km/h results in a larger increase in dynamic forces compared to quasi-static (12.7 % vs 5.8 %). This causes a faster rate of deterioration of track geometry, resulting in an elasticity of −1.55 and a marginal cost of 0.75. The model is also used to investigate the effect of adding extra daily train movements to an existing passenger line. It is shown that additional movements increase the rate of track degradation and marginal costs, particularly if the additional traffic is freight. This is because freight vehicles typically have one only layer of (stiff) suspension, thus generating elevated dynamic forces compared to passenger cars. If two freight trains are added per day it can cause a reduction of the tamping interval of 13 %. Therefore if planning to increase linespeed or add additional freight traffic, the future cost of maintenance should be considered.

CRediT authorship contribution statement

C. Charoenwong: Methodology, Software, Validation, Writing – original draft. **D.P. Connolly:** Conceptualization, Methodology, Resources, Supervision, Writing – original draft, Writing – review & editing. **K. Odolinski:** Methodology, Writing – original draft, Writing – review & editing. **P. Alves Costa:** Supervision. **P. Galvín:** Supervision. **A. Smith:** Supervision.

Declaration of Competing Interest

The authors declare that they have no known competing financial interests or personal relationships that could have appeared to influence the work reported in this paper.

Data availability

The authors do not have permission to share data.

Acknowledgements

The authors are grateful to the University of Leeds, the University of Porto, Seville University and the Leverhulme Trust (PLP-2016-270). This work was partially financed by: Base Funding - UIDB/04708/2020 and Programmatic Funding - UIDP/04708/2020 of the CONSTRUCT - Instituto de I&D em Estruturas e Construções – funded by national funds through the FCT / MCTES (PIDDAC) - Sweden's Innovation Agency (Vinnova). Shift2Rail and IN2TRACK3 are also acknowledged.

Appendix A. Vehicle mass and stiffness matrices.

The track and vehicle compliance are:

$$\{\Delta u(\Omega)\} = \delta u\{b(\Omega)\} \tag{11}$$

$$b(\Omega)_i = e^{i\frac{2\pi}{\lambda}a_i} \tag{12}$$

$$T_c(\Omega) = \frac{1}{2\pi}\int_{-\infty}^{+\infty} u_c^G(k_x,\omega)dk_x \tag{13}$$

$$V^H = \frac{1}{k_H} \tag{14}$$

$$V_c(\Omega) = [Z]\left([K^v] - \Omega^2[M^v]\right)^{-1}[Z]^T \tag{15}$$

where Ω is the driving frequency, defined by $\Omega = \frac{2\pi}{\lambda}v$; T_c is the flexibility term of the track compliance; V_c is the flexibility term of the vehicle compliance; V^H is the contact flexibility matrix; Z is a constant matrix, M^v is the vehicle mass matrix and K^v is the vehicle stiffness.

Mass and stiffness matrices of the passenger vehicle which contains primary and secondary suspensions:

$$[Z] = \begin{bmatrix} 0 & 0 & 0 & 0 & 0 & 0 & 1 & 0 & 0 & 0 \\ 0 & 0 & 0 & 0 & 0 & 0 & 0 & 1 & 0 & 0 \\ 0 & 0 & 0 & 0 & 0 & 0 & 0 & 0 & 1 & 0 \\ 0 & 0 & 0 & 0 & 0 & 0 & 0 & 0 & 0 & 1 \end{bmatrix} \tag{16}$$

$$[M^v] = \begin{bmatrix} Mc & 0 & 0 & 0 & 0 & 0 & 0 & 0 & 0 & 0 \\ 0 & Jc & 0 & 0 & 0 & 0 & 0 & 0 & 0 & 0 \\ 0 & 0 & Mb & 0 & 0 & 0 & 0 & 0 & 0 & 0 \\ 0 & 0 & 0 & Jb & 0 & 0 & 0 & 0 & 0 & 0 \\ 0 & 0 & 0 & 0 & Mb & 0 & 0 & 0 & 0 & 0 \\ 0 & 0 & 0 & 0 & 0 & Jb & 0 & 0 & 0 & 0 \\ 0 & 0 & 0 & 0 & 0 & 0 & Mw & 0 & 0 & 0 \\ 0 & 0 & 0 & 0 & 0 & 0 & 0 & Mw & 0 & 0 \\ 0 & 0 & 0 & 0 & 0 & 0 & 0 & 0 & Mw & 0 \\ 0 & 0 & 0 & 0 & 0 & 0 & 0 & 0 & 0 & Mw \end{bmatrix} \tag{17}$$

$$[K^v] = \begin{bmatrix} 2Ks & 0 & -Ks & 0 & -Ks & 0 & 0 & 0 & 0 & 0 \\ 0 & 2Ks{\cdot}lb^2 & -Ks{\cdot}lb & 0 & Ks{\cdot}lb & 0 & 0 & 0 & 0 & 0 \\ -Ks & -Ks{\cdot}lb & Ks+2Kp & 0 & 0 & 0 & -Kp & -Kp & 0 & 0 \\ 0 & 0 & 0 & 2Kp{\cdot}lw^2 & 0 & 0 & -Kp{\cdot}lw & Kp{\cdot}lw & 0 & 0 \\ -Ks & Ks{\cdot}lb & 0 & 0 & Ks+2Kp & 0 & 0 & 0 & -Kp & -Kp \\ 0 & 0 & 0 & 0 & 0 & 2Kp{\cdot}lw^2 & 0 & 0 & -Kp{\cdot}lw & Kp{\cdot}lw \\ 0 & 0 & -Kp & -Kp{\cdot}lw & 0 & 0 & Kp & 0 & 0 & 0 \\ 0 & 0 & -Kp & Kp{\cdot}lw & 0 & 0 & 0 & Kp & 0 & 0 \\ 0 & 0 & 0 & 0 & -Kp & -Kp{\cdot}lw & 0 & 0 & Kp & 0 \\ 0 & 0 & 0 & 0 & -Kp & Kp{\cdot}lw & 0 & 0 & 0 & Kp \end{bmatrix} \tag{18}$$

Mass and stiffness matrices of the freight vehicle which contains only one set of suspension:

$$[Z] = \begin{bmatrix} 0 & 0 & 1 & lw & 0 & 0 \\ 0 & 0 & 1 & -lw & 0 & 0 \\ 0 & 0 & 0 & 0 & 1 & lw \\ 0 & 0 & 1 & 0 & 1 & -lw \end{bmatrix} \tag{19}$$

$$[M^v] = \begin{bmatrix} Mc & 0 & 0 & 0 & 0 & 0 \\ 0 & Jc & 0 & 0 & 0 & 0 \\ 0 & 0 & Mb+2Mw & 0 & 0 & 0 \\ 0 & 0 & 0 & Jb+2Mw{\cdot}lw^2 & 0 & 0 \\ 0 & 0 & 0 & 0 & Mb+2Mw & 0 \\ 0 & 0 & 0 & 0 & 0 & Jb+2Mw{\cdot}lw^2 \end{bmatrix} \tag{20}$$

$$[K^v] = \begin{bmatrix} 2Ks & 0 & -Ks & 0 & -Ks & 0 \\ 0 & 2Ks{\cdot}lb^2 & -Ks{\cdot}lb & 0 & Ks{\cdot}lb & 0 \\ -Ks & -Ks{\cdot}lb & Ks & 0 & 0 & 0 \\ 0 & 0 & 0 & 0 & 0 & 0 \\ -Ks & Ks{\cdot}lb & 0 & 0 & Ks & 0 \\ 0 & 0 & 0 & 0 & 0 & 0 \end{bmatrix} \tag{21}$$

where Mc is mass of the car box; Mb is mass of the bogie; Mw is mass of the wheelset; Jb is the rotational inertia of the car body; Kp is the complex stiffness of the primary suspension; Ks is the complex stiffness of the secondary suspension; lb is half the distance between the bogie's centre of gravity; and lw is half the wheelbase that shares the same bogie. Kp and Ks are defined as:

$$Kp = k_{pri} + i\omega c_{pri} \tag{22}$$

$$Ks = k_{sec} + i\omega c_{sec} \tag{23}$$

where k_{pri} is the spring stiffness of the primary suspension; k_{sec} is the spring stiffness of the secondary suspension; c_{pri} is the viscous damping of the primary suspension; and k_{sec} is the viscous damping of the secondary suspension.

Appendix B. . Ballasted track properties (validation case)

Component	Parameter	Value
UIC 60 Rail (single rail)	Height (m)	0.172
	Length in transversal direction (m)	0.015
	Section area (m^2)	7.677×10^{3}
	Moment of Inertia y-y (m^4)	3.038×10^{-5}
	Moment of Inertia z-z (m^4)	0.512×10^{-5}
	Young's modulus (Pa)	2.11×10^{11}
	Density (kg/m^3)	7850
	Poisson's ratio	0.3
	Hysteric damping coefficient	0.01
Railpad (spring element)	Continuous stiffness (N/m^2)	255×10^{6}
	Viscous damping (Ns^2/m^2)	22.5×10^{3}
Sleeper (G44)	Height (m)	0.2

(continued on next page)

(*continued*)

Component	Parameter	Value
	Length in transversal direction (m)	2.5
	Sleeper spacing (m)	0.65
	Young's modulus (Pa)	3×10^{10}
	Density (kg/m^3)	2500
	Poisson's ratio	0.15
	Hysteric damping coefficient	0.01
Ballast	Height (m)	0.3
	Length in transversal direction (m)	2.8
	Young's modulus (Pa)	180×10^6
	Density (kg/m^3)	1600
	Poisson's ratio	0.27
	Hysteric damping coefficient	0.061
Sub-ballast	Height (m)	0.5
	Length in transversal direction (m)	3.5
	Young's modulus (Pa)	212×10^6
	Density (kg/m^3)	1913
	Poisson's ratio	0.3
	Hysteric damping coefficient	0.054
Subgrade layer 1	Height (m)	0.5
	Young's modulus (Pa)	30×10^6
	Density (kg/m^3)	2000
	Poisson's ratio	0.3
	Hysteric damping coefficient	0.03
	Settlement parameter a	0.64
	Settlement parameter b	0.10
	Settlement parameter m	1.70
	Compressive strength (kPa)	100
Subgrade layer 2	Height (m)	5
	Young's modulus (Pa)	80×10^6
	Density (kg/m^3)	2000
	Poisson's ratio	0.3
	Hysteric damping coefficient	0.03
	Settlement parameter a	0.64
	Settlement parameter b	0.10
	Settlement parameter m	1.70
	Compressive strength (kPa)	220

References

[1] Fröhling RD. Prediction of Spatially Varying Track Settlement. Conf Railw Eng 1998;CORE98:103–9.

[2] Kawaguchi A, Miwa M, Terada K. Actual data analysis of alignment irregularity growth and its prediction model. Q Rep RTRI (Railw Tech Res Institute) 2005;46 (4):262–8. https://doi.org/10.2219/rtriqr.46.262.

[3] Sharma S, Cui Y, He Q, Mohammadi R, Li Z. Data-driven optimization of railway maintenance for track geometry. Transp Res Part C Emerg Technol 2018;90:34–58. https://doi.org/10.1016/j.trc.2018.02.019.

[4] Bai L, Liu R, Sun Q, Wang F, Xu P. Markov-based model for the prediction of railway track irregularities. Proc Inst Mech Eng Part F J Rail Rapid Transit 2015; 229(2):150–9. https://doi.org/10.1177/0954409713503460.

[5] Vale CM, Lurdes S. Stochastic model for the geometrical rail track degradation process in the Portuguese railway Northern Line. Reliab Eng Syst Saf 2013; 116: 91–8. Doi: 10.1016/j.ress.2013.02.010.

[6] Ali L, Amin S, Wehbi M. Backpropagation algorithms of neural networks to construct the railway track deterioration model. In: 2021 7th Int Conf Model Technol Intell Transp Syst MT-ITS 2021 2021. Doi: 10.1109/MT-ITS49943.2021.9529272.

[7] Sasidharan M, Burrow MPN, Ghataora GS, Marathu R. A risk-informed decision support tool for the strategic asset management of railway track infrastructure. Proc Inst Mech Eng Part F J Rail Rapid Transit 2022;236(2):183–97. https://doi.org/10.1177/09544097211038373.

[8] Guo Y, Zhai W. Long-term prediction of track geometry degradation in high-speed vehicle–ballastless track system due to differential subgrade settlement. Soil Dyn Earthq Eng 2018;113:1–11. https://doi.org/10.1016/j.soildyn.2018.05.024.

[9] Nielsen JCO, Li X. Railway track geometry degradation due to differential settlement of ballast/subgrade – Numerical prediction by an iterative procedure. J Sound Vib 2018;412:441–56. https://doi.org/10.1016/j.jsv.2017.10.005.

[10] Grossoni I, Powrie W, Zervos A, Bezin Y, Le Pen L. Modelling railway ballasted track settlement in vehicle-track interaction analysis. Transp Geotech 2021;26: 100433. https://doi.org/10.1016/j.trgeo.2020.100433.

[11] Kumar N, Kossmann C, Scheriau S, Six K. An efficient physical-based method for predicting the long-term evolution of vertical railway track geometries. Proc Inst Mech Eng Part F J Rail Rapid Transit 2022;236(4):447–65. https://doi.org/10.1177/09544097211024803.

[12] Connolly DP, Dong K, Alves Costa P, Soares P, Woodward PK. High speed railway ground dynamics: a multi-model analysis. Int J Rail Transp 2020;8(4):324–46. https://doi.org/10.1080/23248378.2020.1712267.

[13] Connolly DP, Costa PA. Geodynamics of very high speed transport systems. Soil Dyn Earthq Eng 2020;130:105982. https://doi.org/10.1016/j.soildyn.2019.105982.

[14] Chumyen P, Connolly DP, Woodward PK, Markine V. The effect of soil improvement and auxiliary rails at railway track transition zones. Soil Dyn Earthq Eng 2022;155:107200. https://doi.org/10.1016/j.soildyn.2022.107200.

[15] Ramos A, Gomes Correia A, Calçada R, Alves Costa P. Stress and permanent deformation amplification factors in subgrade induced by dynamic mechanisms in track structures. Int J Rail Transp 2022;10(3):298–330. https://doi.org/10.1080/23248378.2021.1922317.

[16] Alves Costa P, Lopes P, Silva CA. Soil shakedown analysis of slab railway tracks: Numerical approach and parametric study. Transp Geotech 2018;16:85–96. https://doi.org/10.1016/j.trgeo.2018.07.004.

[17] Li D, Selig ET. Cumulative Plastic Deformation for Fine-Grained Subgrade Soils. J Geotech Eng 1996;122(12):1006–13.

[18] Dahlberg T. Some railroad settlement models - A critical review. Proc Inst Mech Eng Part F J Rail Rapid Transit 2001;215(4):289–300. https://doi.org/10.1243/0954409011531585.

[19] Suiker ASJ, de Borst R. A numerical model for the cyclic deterioration of railway tracks. Int J Numer Methods Eng 2003;57(4):441–70. https://doi.org/10.1002/nme.683.

[20] Indraratna B, Thakur PK, Vinod JS, Salim W. Semiempirical Cyclic Densification Model for Ballast Incorporating Particle Breakage. Int J Geomech 2012;12(3): 260–71.

[21] Shih J-Y, Grossoni I, Bezin Y. Settlement analysis using a generic ballasted track simulation package. Transp Geotech 2019;20:100249. https://doi.org/10.1016/j.trgeo.2019.100249.

[22] Guo Y, Zhao C, Markine V, Jing G, Zhai W. Calibration for discrete element modelling of railway ballast: A review. Transp Geotech 2020;23:100341. https://doi.org/10.1016/j.trgeo.2020.100341.

[23] Saussine G, Cholet C, Gautier PE, Dubois F, Bohatier C, Moreau JJ. Modelling ballast behaviour under dynamic loading. Part 1: A 2D polygonal discrete element method approach. Comput Methods Appl Mech Eng 2006;195(19-22):2841–59. https://doi.org/10.1016/j.cma.2005.07.006.

[24] Shenton MJ. Ballast deformation and track deterioration. Track Technol 1985: 253–65.

[25] ORE. Question D71: Stresses in the Rails, the Ballast and in the Formation Resulting from Traffic Loads. Stresses in the formation (results of the third phase ; measurements under dynamic conditions). International Union of Railways, Office for Research and Experiments; 1970.
[26] Sato Y. Japanese Studies on Deterioration of Ballasted Track. Veh Syst Dyn 1995;24 (sup1):197–208. https://doi.org/10.1080/00423119508969625.
[27] Indraratna B, Nimbalkar S. Stress-Strain Degradation Response of Railway Ballast Stabilized with Geosynthetics. J Geotech Geoenviron Eng 2013;139(5):684–700.
[28] Menan Hasnayn M, John McCarter W, Woodward PK, Connolly DP, Starrs G. Railway subgrade performance during flooding and the post-flooding (recovery) period. Transp Geotech 2017;11:57–68. https://doi.org/10.1016/j.trgeo.2017.02.002.
[29] Yu Z, Woodward PK, Laghrouche O, Connolly DP. True triaxial testing of geogrid for high speed railways. Transp Geotech 2019;20:100247. https://doi.org/10.1016/j.trgeo.2019.100247.
[30] Li BD, Member A, Selig ET. Resilient modulus for fine – grained. 1994; 120: 939–57.
[31] Liu J, Xiao J. Experimental Study on the Stability of Railroad Silt Subgrade with Increasing Train Speed. J Geotech Geoenviron Eng 2010;136(6):833–41.
[32] Sayeed MA, Shahin MA. Design of ballasted railway track foundations using numerical modelling. Part I: Development1. Can Geotech J 2018;55(3):353–68. https://doi.org/10.1139/cgj-2016-0633.
[33] Chen C, McDowell GR. An investigation of the dynamic behaviour of track transition zones using discrete element modelling. Proc Inst Mech Eng Part F J Rail Rapid Transit 2016;230(1):117–28. https://doi.org/10.1177/0954409714528892.
[34] Shan Y, Zhou S, Zhou H, Wang B, Zhao Z, Shu Y, et al. Iterative method for predicting uneven settlement caused by high-speed train loads in transition-zone subgrade. Transp Res Rec 2017;2607(1):7–14. https://doi.org/10.3141/2607-02.
[35] Ramos A, Gomes Correia A, Indraratna B, Ngo T, Calçada R, Costa PA. Mechanistic-empirical permanent deformation models: Laboratory testing, modelling and ranking. Transp Geotech 2020;23:100326. https://doi.org/10.1016/j.trgeo.2020.100326.
[36] Yan T-H, Corman F. Assessing and Extending Track Quality Index for Novel Measurement Techniques in Railway Systems. Transp Res Rec 2020;2674(8): 24–36. https://doi.org/10.1177/0361198120923661.
[37] Neuhold J, Landgraf M, Marschnig S, Veit P. Measurement Data-Driven Life-Cycle Management of Railway Track. Transp Res Rec 2020;2674(11):685–96. https://doi.org/10.1177/0361198120946007.
[38] Charoenwong C, Connolly DP, Woodward PK, Galvín P, Alves Costa P. Analytical forecasting of long-term railway track settlement. Comput Geotech 2022;143: 104601. https://doi.org/10.1016/j.compgeo.2021.104601.
[39] Smith ASJ, Odolinski K, Hossein-Nia S, Jönsson P-A, Stichel S, Iwnicki S, et al. Estimating the marginal maintenance cost of different vehicle types on rail infrastructure. Proc Inst Mech Eng Part F J Rail Rapid Transit 2021;235(10): 1191–202. https://doi.org/10.1177/0954409721991309.
[40] Dong K, Connolly DP, Laghrouche O, Woodward PK, Alves CP. Non-linear soil behaviour on high speed rail lines. Comput Geotech 2019;112:302–18. https://doi.org/10.1016/j.compgeo.2019.03.028.
[41] Alves Costa P, Calçada R, Silva Cardoso A, Bodare A. Influence of soil non-linearity on the dynamic response of high-speed railway tracks. Soil Dyn Earthq Eng 2010; 30(4):221–35. https://doi.org/10.1016/j.soildyn.2009.11.002.
[42] Yoshida N, Kobayashi S, Suetomi I, Miura K. Equivalent linear method considering frequency dependent characteristics of stiffness and damping. Soil Dyn Earthq Eng 2002;22(3):205–22. https://doi.org/10.1016/S0267-7261(02)00011-8.
[43] Fernández-Ruiz J, Castanheira-Pinto A, Costa PA, Connolly DP. Influence of non-linear soil properties on railway critical speed. Constr Build Mater 2022;335: 127485. https://doi.org/10.1016/j.conbuildmat.2022.127485.
[44] Zhai W. Vehicle–Track Coupled Dynamics Models. Veh. Coupled Dyn. Theory Appl., Singapore: Springer Singapore; 2020, p. 17–149. Doi: 10.1007/978-981-32-9283-3_2.
[45] Colaço A, Costa PA, Connolly DP. The influence of train properties on railway ground vibrations. Struct Infrastruct Eng 2016;12(5):517–34. https://doi.org/10.1080/15732479.2015.1025291.
[46] Costa PA, Calçada R, Cardoso AS. Influence of train dynamic modelling strategy on the prediction of track-ground vibrations induced by railway traffic. Proc Inst Mech Eng Part F J Rail Rapid Transit 2012;226(4):434–50. https://doi.org/10.1177/0954409711433686.
[47] Lamprea-Pineda AC, Connolly DP, Hussein MFM. Beams on elastic foundations – A review of railway applications and solutions. Transp Geotech 2022;33:100696. https://doi.org/10.1016/j.trgeo.2021.100696.
[48] Federal Railroad Administration. Statistical Representations of Track Geometry : Volume I. Washington, D.C.; 1980.
[49] Kouroussis G, Connolly DP, Verlinden O. Railway-induced ground vibrations – a review of vehicle effects. Int J Rail Transp 2014;2(2):69–110. https://doi.org/10.1080/23248378.2014.897791.
[50] Sheng X. Ground vibrations generated from trains. University of Southampton; 2001.
[51] Andersson M, Björklund G, Haraldsson M. Marginal railway track renewal costs: A survival data approach. Transp Res Part A Policy Pract 2016;87:68–77. https://doi.org/10.1016/j.tra.2016.02.009.
[52] Öberg J, Andersson E, Gunnarsson J. Track access charging with respect to vehicle characteristics. Rapp LA-BAN 2007;31:2007.
[53] ECOPLAN/IMDM. Modelling railway infrastructure maintenance and renewal costs in France. Overview of estimates. Final report. (Mimeo); 2020.